Supporting Information:

ATR FTIR and ^{1}H NMR of GNP surface ligands

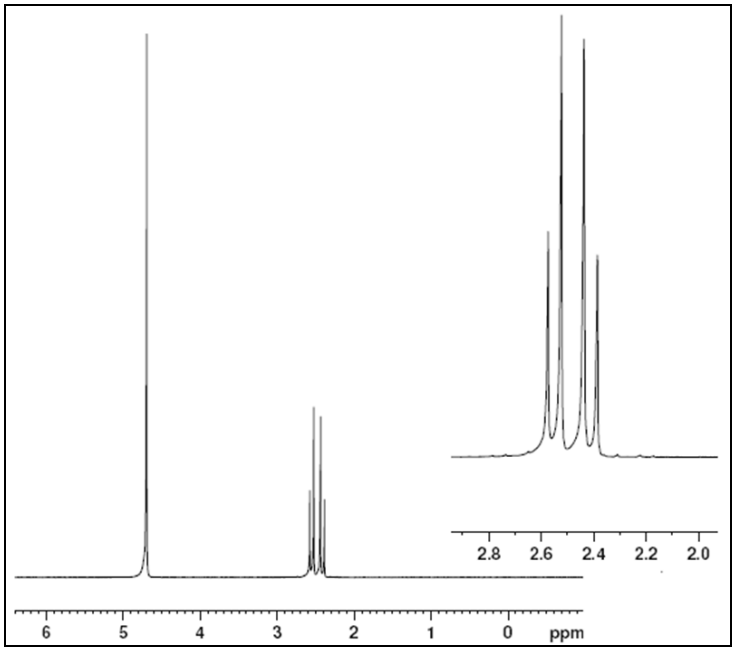

Figure S1: ^{1}H NMR spectrum of pure Sodium Citrate Dihydrate in D_2O.

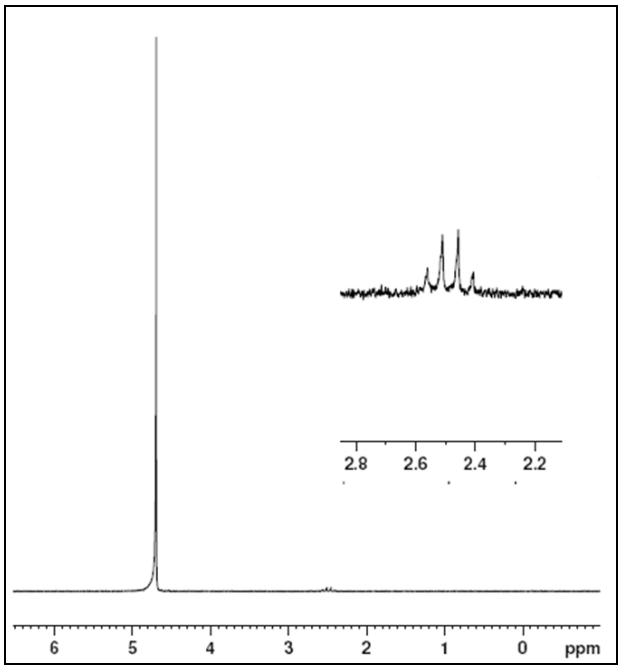

Figure S2: ^{1}H NMR spectrum of Sodium Citrate Dihydrate capped AuNP's in D_2O after 2 washes to remove excess citrate.

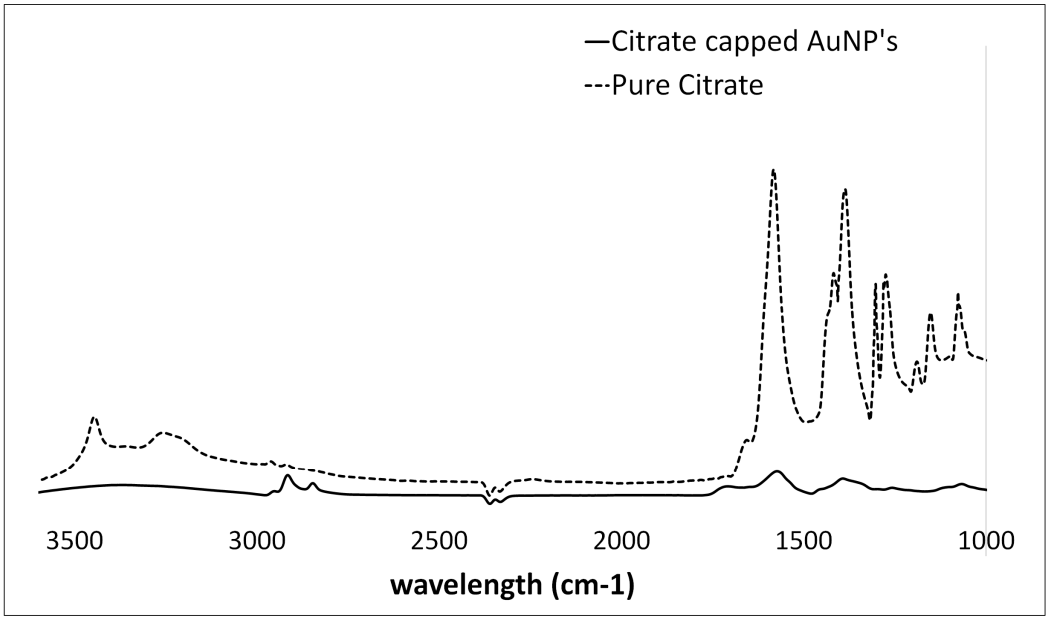

Figure S3. ATR FT-IR spectra of Pure Sodium Citrate Dihydrate Vs AuNP's capped by the citrate ligand after 2 washes.

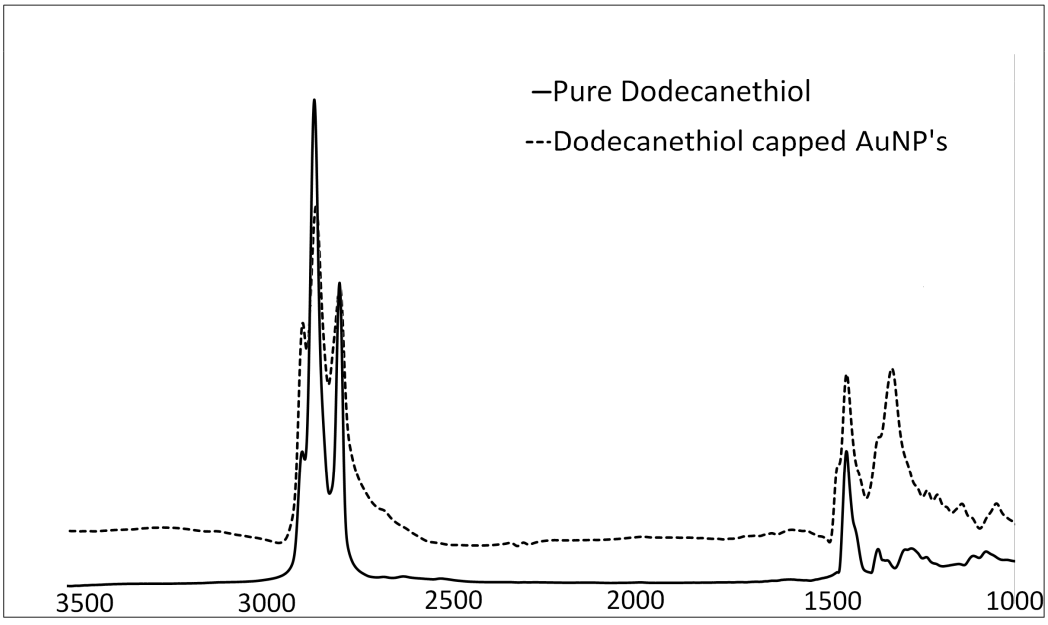

Figure S4: ATR FT-IR spectra of pure dodecanethiol and dodecanethiol capped GNPs after 2 washes to remove excess ligand

The precipitation of GNPs (stabilized by citrate and before ligand exchange with dodecanethiol) followed by centrifugation and subsequent drying resulted in spectrum that could be well correlated with the spectrum of pure sodium citrate. This would be expected for samples of GNPs which are completely dry, since the solid residue only contains the citrate molecules attached to the surface of the NPs while other more volatile and unstable ketone compounds are removed during the drying process.

This is supported by Ojea-Jime´nez et. al.(*J. Phys. Chem. C*, 2010, 114 (4), pp 1800–1804), who postulate that ketone compounds which arise from the decarboxylation of the citrate can lead to unwanted peaks in the FT IR spectrum. This was found in this work when samples were in solution or not sufficiently dried. But despite drying samples for 1 hr in the vacuum oven at 30 psig and at 60 deg. C, there was still some slight evidence of CH_3 and CH_2 functionality in our citrate capped particles. This along with the slight absorbance at ~1700 $cm^{-}1$ shows that a ketone compound may have been present along with residual solvent, but our particles have a majority of citrate on the surface.

Following ligand exchange and 2 washing cycles, the FTIR spectra demonstrate an absence of citrate within the detectable limits and a presence of dodecanethiol as the predominant ligand. ^{1}H NMR confirms the absence of citrate and confinement of the dodecanethiol to the nanoparticle surface, shown by peak broadening and the disappearance of the A protons below.

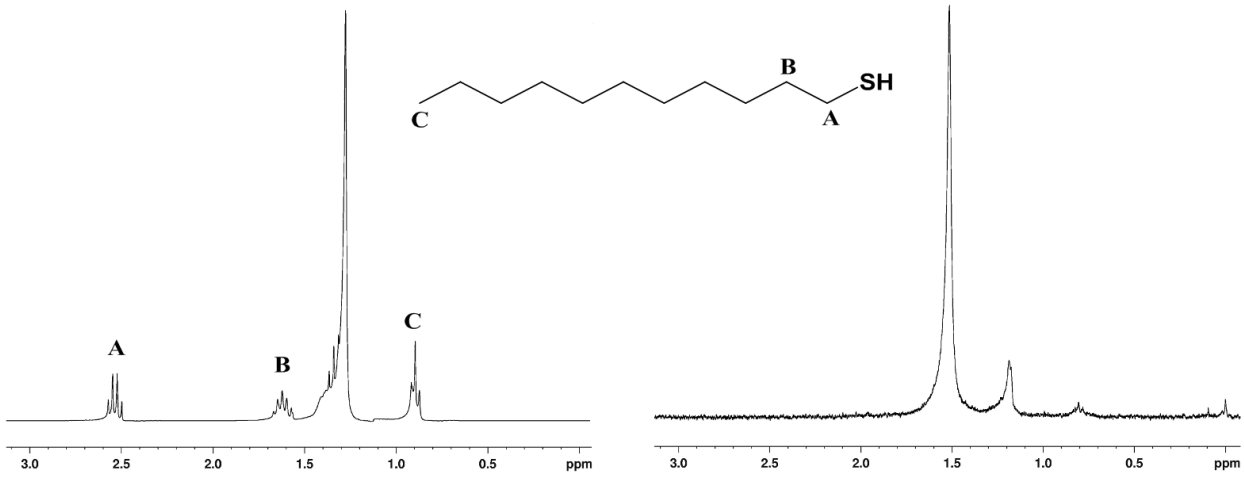

Figure S5: ^{1}H NMR spectra of pure dodecanethiol in $CDCl_3$ vs dodecanethiol capped GNPs after 2 washes to remove excess ligand in $CDCl_3$

According to Canzi et. al. (*J. Phys. Chem. C*, 2011, 115 (16), pp 7972–7978), the large line broadening as well as the absence of significant peaks is significant evidence of surface attachment and absence of unbound excess dodecanethiol in solution.

SANS Results – Additional plots of results and fit SANS spectra.

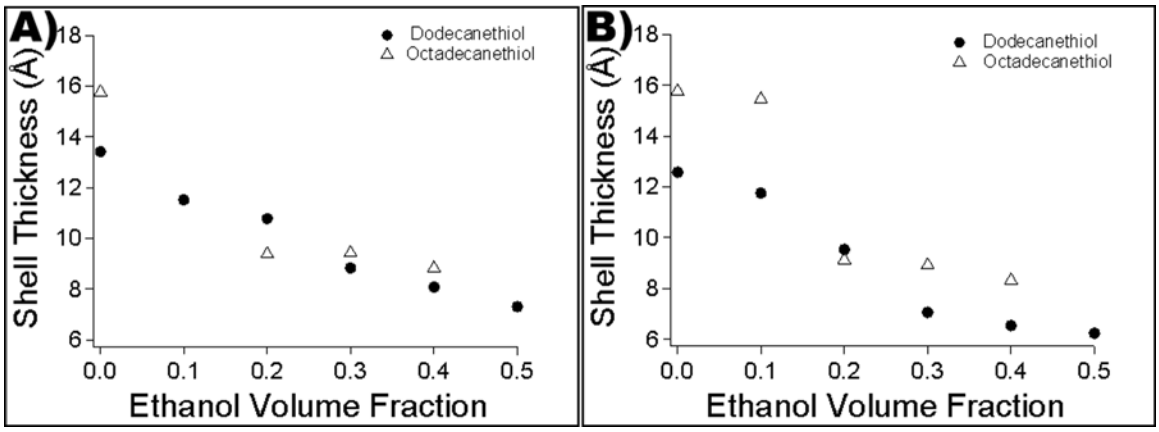

Figure S6: Dodecanethiol and octadecanethiol ligand shell thickness plotted as a function of ethanol-*d6* volume fraction for gold nanoparticles dispersed in A) *n*-hexane-d_{14} and B) toluene-d_8.

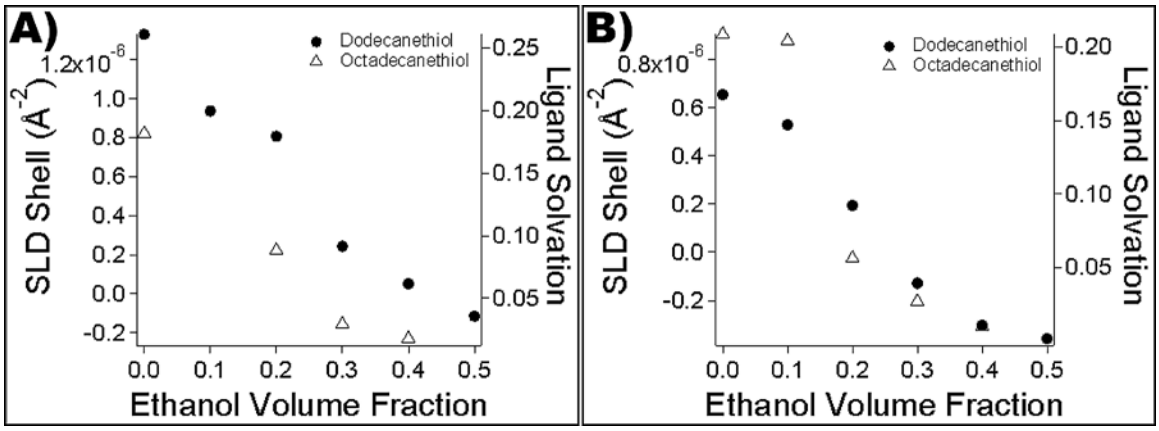

Figure S7: The shell scattering length density (SLD_{shell}) and ligand solvation plotted as a function ethanol-d_6 volume fraction for dodecanethiol and octadecanethiol stabilized gold nanoparticles dispersed in A) *n*-hexane-d_{14} and B) toluene-d_8.

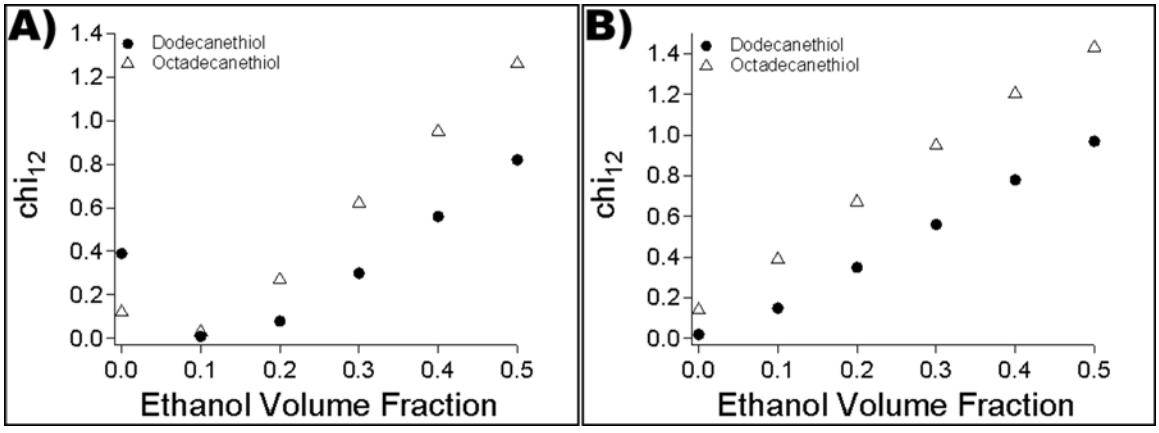

Figure S8: Calculated χ_{12} Flory-Huggins interaction parameter for dodecanethiol and octadecanethiol in the A) *n*-hexane-d_{14}/ethanol-d_6 and B) toluene-d_8/ethanol-d_6 solvent mixtures.

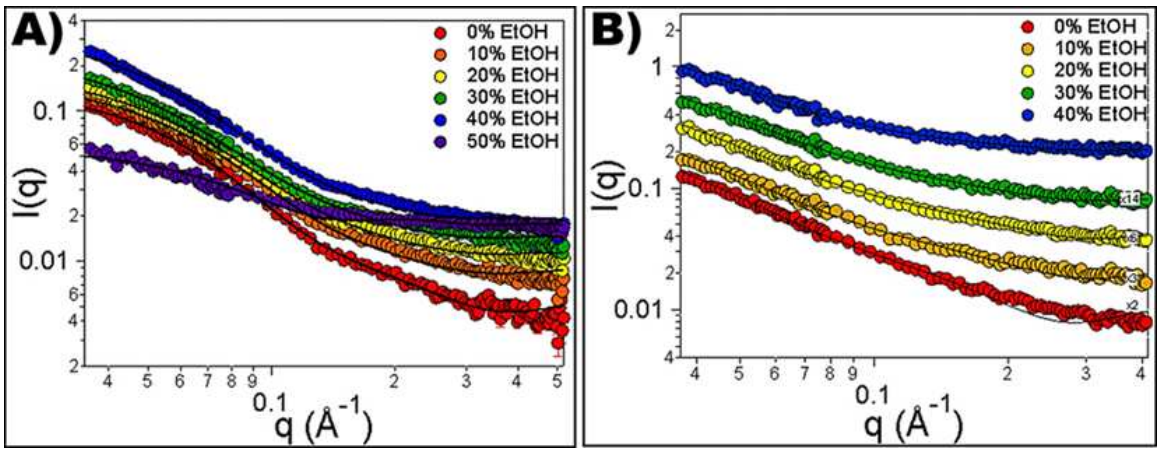

Figure S9: Fit SANS data for A) dodecanethiol and B) octadecanethiol capped gold nanoparticles dispersed in toluene-d_8 with varying ethanol-d_6 composition fit using a polydisperse core-shell model. Some of the scattering spectra have been offset for clarity.

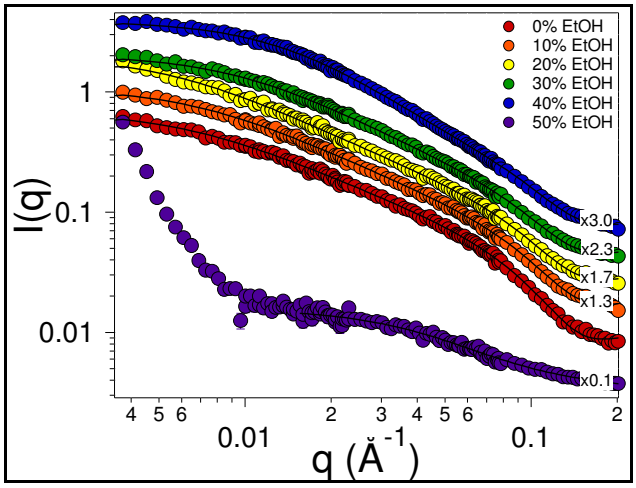

Figure S10: Fit SANS data for dodecanethiol modified gold nanoparticles dispersed in toluene-d_8 using a fractal model. The scattering spectra have been offset for clarity.